Self-Deployment Algorithms for Field Coverage in a Network of Nonidentical Mobile Sensors

Hamid Mahboubi, Kaveh Moezzi, Amir G. Aghdam and Kamran Sayrafian-Pour

***Abstract*— In this paper, efficient deployment algorithms are proposed for a mobile sensor network to improve coverage. The proposed algorithms calculate the position of the sensors iteratively based on the existing coverage holes in the target field. The multiplicatively weighted Voronoi diagram (MW-Voronoi diagram) is used to discover the coverage holes corresponding to different sensors with different sensing ranges. The algorithms proposed in this paper consider the distances of each sensor and the points inside its corresponding MW-Voronoi region from the boundary curves of the region. Under the proposed algorithms, the sensors move in such a way that the coverage holes in the target field are reduced. Simulations confirm the effectiveness of the deployment algorithms proposed in this paper.**

I. Introduction

Wireless sensor networks have received a great deal of attention in recent years, due to their increasing capabilities in a wide range of applications. Such applications include environmental monitoring, military surveillance and outer space exploration, to name only a few [1], [2], [3], [4]. The main challenge in the design of efficient sensor networks is to optimize coverage and resource allocation [5], [6]. On the other hand, there are some practical constraints that need to be taken into account in developing sensor deployment strategies. For example, due to the distributed nature of the network, it is often desired to design a decentralized resource allocation protocol [6]. Furthermore, in many applications the initial positions of the sensors are not known *a priori* [7].

In [8], location services (which are concerned with obtaining the location information of the destination) for mobile ad-hoc networks are reviewed. A new coverage model (namely, surface coverage) is proposed in [9], and two pertinent problems concerning (i) expected coverage ratio with stochastic deployment , and (ii) optimal deployment strategy with planned deployment are subsequently investigated. Furthermore, three approximation algorithms with provable approximation ratios are introduced in [9]. Several sensor deployment strategies are proposed in the literature for mobile sensors to provide sufficient coverage in the field [6], [10], [11], [12], [13], [14]. In these works, it is mainly assumed that all sensors have the same sensing range. However, this is not a realistic assumption in many real-world applications.

In this work, a number of distributed sensor deployment strategies are introduced for a network of mobile sensors with different sensing ranges. The multiplicatively weighted Voronoi (MW-Voronoi) is used to divide the region into a number of cells, where the weight assigned to each sensor is proportional to its sensing radius [15], [16], [17]. The resultant diagram is subsequently used to find the coverage holes in the network. Three algorithms are proposed in this work to improve network coverage: Maxmin-curve, Minmax-curve and Curtex. The main characteristic of these algorithms is that the sensor movement is performed iteratively. Once each destination is computed, new local coverage area of the corresponding sensor (in the previously constructed MW-Voronoi region) is compared to its preceding local coverage area. If the new local coverage area is larger than the preceding one, the sensor moves to the new destination; otherwise, it remains in its current position. If, on the other hand, the local coverage area of every sensor in an iteration is not increased by a certain threshold, the algorithm is terminated (to ensure a finite number of iterations).

The rest of the paper is organized as follows. In Section II, some preliminaries as well as important notions and definitions are provided. Section III presents three different techniques for efficient network coverage, as the main contribution of the paper. Simulation results are given in Section IV to demonstrate the effectiveness of the proposed approaches, and finally the concluding remarks are summarized in Section V.

II. Background

Let $\mathbf{S}$ be a set of n distinct weighted nodes in the plane denoted by $(S_1, w_1), (S_2, w_2), \ldots, (S_n, w_n)$, where $w_i > 0$ is the weighting factor associated with S_i, for any $i \in \mathbf{n} := \{1, 2, \ldots, n\}$. Partition the plane into n regions such that:

- Each region contains only one node, and
- the nearest node, in the sense of weighted distance, to any point inside a region is the node assigned to that region.

The diagram obtained by the partitioning described above is called the *multiplicatively weighted Voronoi diagram* (MW-Voronoi diagram) [16]. Analogous to conventional Voronoi diagram, the mathematical characterization of each region obtained by the above partitioning is as follows:

$$\bar{\Pi}_i = \left\{ Q \in \mathbb{R}^2 \mid w_j d(Q, S_i) \leq w_i d(Q, S_j), \forall j \in \mathbf{n} - \{i\} \right\} \tag{1}$$

for any $i \in \mathbf{n}$, where $d(Q, S_i)$ is the Euclidean distance between Q and S_i.

According to (1), any point Q in the i-th MW-Voronoi region $\bar{\Pi}_i$ has the following property:

$$\frac{d(Q, S_i)}{d(Q, S_j)} \leq \frac{w_i}{w_j}, \quad \forall i \in \mathbf{n},\ \forall j \in \mathbf{n} - \{i\} \tag{2}$$

Definition 1. Similar to conventional Voronoi diagram, the nodes S_i and S_j $(i, j \in \mathbf{n}, i \neq j)$ in an MW-Voronoi diagram are called neighbors if $\bar{\Pi}_i \cap \bar{\Pi}_j \neq \emptyset$. The set of all neighbors of S_i, $i \in \mathbf{n}$, is denoted by $\mathbf{N}_i$ and is formulated below:

$$\mathbf{N}_i = \left\{ S_j \in \mathbf{S} \mid \bar{\Pi}_i \cap \bar{\Pi}_j \neq \emptyset,\ \forall j \in \mathbf{n} \right\} \tag{3}$$

Definition 2. Consider a sensor S_i with the sensing radius r_i and the corresponding MW-Voronoi region $\bar{\Pi}_i$, $i \in \mathbf{n}$, and let Q be an arbitrary point inside $\bar{\Pi}_i$. The intersection of the region $\bar{\Pi}_i$ and a circle of radius r_i centered at Q is referred to as the *coverage area with respect to (w.r.t.) Q*. The coverage

H. Mahboubi, K. Moezzi and A. G. Aghdam are with the Department of Electrical & Computer Engineering, Concordia University, 1455 de Maisonneuve Blvd. W., EV005.139, Montréal, Québec H3G 1M8 Canada, {h_mahbo,k_moezz,aghdam}@ece.concordia.ca

K. Sayrafian-Pour is with the National Institute of Standards and Technology (NIST), 100 Bureau Drive, Stops 8920 and 8910 Gaithersburg, MD 20899 USA {ksayrafian}@nist.gov

This work has been supported by the National Institute of Standards and Technology (NIST), under grant 70NANB8H8146.

area w.r.t. the location of the sensor S_i is called the *local coverage area* of that sensor.

Definition 3. The *Apollonian circle* of the segment AB, denoted by $\Omega_{AB,k}$, is the locus of all points E such that $\frac{AE}{BE} = k$ [18].

To construct the i-th MW-Voronoi region, first the Apollonian circles of the neighboring partitions are found for the i-th sensor. In other words, the Apollonian circles $\Omega_{S_iS_j,\frac{w_i}{w_j}}$ are found for all $S_j \in \mathbf{N}_i$. The smallest region (created by the above circles) containing the i-th node is, in fact, the i-th MW-Voronoi region (e.g., see Fig. 1). An example of a MW-Voronoi diagram with 15 sensors is sketched in Fig. 2.

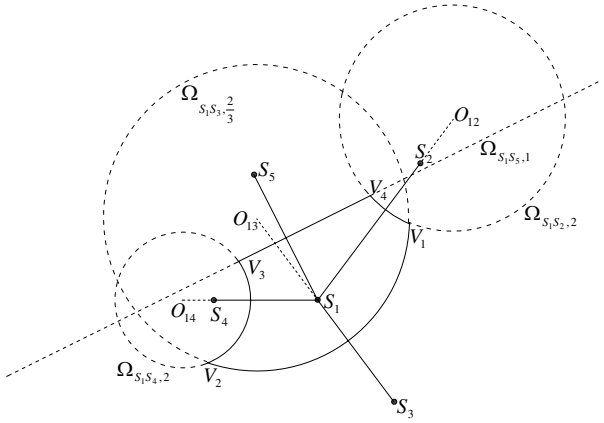

Fig. 1. The MW-Voronoi region for a sensor S_1 with four neighbors $S_2, \ldots, S_5$.

The MW-Voronoi diagram is the main tool for sensor deployment in this paper. Each sensor has a sensing area which is a circle whose size can be different for distinct sensors. Let each sensor in the field be denoted by a node with a weight equal to its sensing radius, and sketch the MW-Voronoi region for each sensor. From the characterization of the MW-Voronoi regions provided in (1), it is straightforward to show that if a sensor cannot detect a phenomenon in its corresponding region, no other sensor can detect it either. This means that in order to find the "so-called" coverage holes (i.e., the undetectable points in the network), it would suffice to compare the MW-Voronoi region of each node with its local coverage area.

Notation 1. Consider a circle of radius r centered at O, denoted by $\Omega(O, r)$ hereafter, and a point V in the plane. The intersections of Ω and the extension of VO from O is denoted by $T^V_{\Omega(O,r)}$. The other intersection point of $\Omega(O, r)$ and VO (or its extension) is denoted by $\bar{T}^V_{\Omega(O,r)}$.

Notation 2. As mentioned before, the boundary curves of an MW-Voronoi region are the segments of some Apollonian circles. The set of all such Apollonian circles for the i-th MW-Voronoi region is denoted by $\mathbf{\Omega}_i$. The sets $\bar{\mathbf{\Omega}}_i$ and $\tilde{\mathbf{\Omega}}_i$ are then defined as follows:

$$\bar{\mathbf{\Omega}}_i = \{\Omega \in \mathbf{\Omega}_i | S_i \in \Omega\}$$

$$\tilde{\mathbf{\Omega}}_i = \{\Omega \in \mathbf{\Omega}_i | S_i \notin \Omega\}$$

Assumption 1. In this paper, it is assumed that there is no obstacle in the field. Therefore, the sensors can move to any desired location without obstacle avoidance concerns using existing techniques, e.g. [11], [12], [19], [20].

Assumption 2. The sensors are supposed to be capable of localizing themselves with sufficient accuracy in the field (using, for instance, the methods proposed in [1], [21]).

Assumption 3. The communication range of the sensors is bounded (and not necessarily the same for all sensors). This is a limiting factor for the sensors, potentially preventing them from reaching their neighbors, which can result in incorrect Voronoi regions around some of the sensors. Consequently, such a limitation can negatively affect the detection of coverage holes.

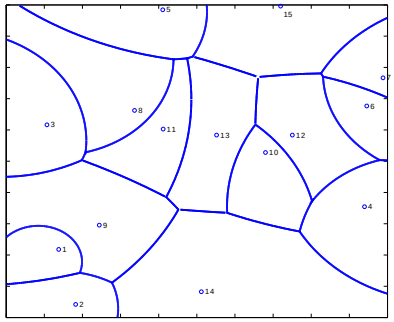

Fig. 2. An example of the MW-Voronoi diagram for a group of 15 nonidentical sensors in a network.

III. Deployment Protocols

In this section, three different protocols are developed for a distributed sensor network. The proposed algorithms are iterative, where in each iteration every sensor first broadcasts its sensing radius and location to other sensors, and then constructs its MW-Voronoi region based on the received information. It checks the region subsequently to detect the possible coverage holes. If any coverage hole exists, the sensor calculates its target location (but does not move there) in such a way that by moving there the coverage hole would be eliminated, or at least its size would be reduced by a certain threshold. Once the new target location is calculated, the coverage area w.r.t. this location (in the previously constructed MW-Voronoi region) is obtained. If this coverage area is greater than the current one, the sensor moves to the new location; otherwise, it remains in its current position. In order to terminate the algorithm in finite time, a proper coverage improvement threshold ϵ is defined such that if the increase in the local coverage area by each sensor is not sufficiently large (as specified by ϵ), there is no need to continue the iterations.

Notation 3. In the remainder of this paper, $\mathcal{V}$ represents an MW-Voronoi diagram with n regions (each one corresponding to a node). Furthermore, the number of vertices and boundary curves of the i-th region are denoted by m_i, and e_i, respectively. It is easy to verify that $m_i = e_i$, for the case when the corresponding region has at least two vertices.

Definition 4. The corner points of the i-th MW-Voronoi region (i.e., the intersection points of its boundary curves) are denoted by $\mathbf{V}_i = \{V_{i1}, V_{i2}, \ldots, V_{il}\}$. These points are called the MW-Voronoi vertices for the i-th region. It is to be noted that in any MW-Voronoi region, the farthest point from the node associated with that region lies on its boundary.

A. Minmax-Curve Strategy

The idea behind the Minmax-curve technique is that normally for optimal coverage, each sensor should not be too far from any of the boundary curves in its MW-Voronoi region. The Minmax-curve strategy selects the target location

for each sensor as a point inside the corresponding MW-Voronoi region whose distance from the farthest curve is minimized. This point will be referred to as the *Minmax-curve centroid*, and will be denoted by $\acute{O}_i$ for the i-th region, $i \in \mathbf{n}$. Furthermore, the distance between this point and the farthest curve from it will be represented by $\acute{r}_i$. The Minmax-curve circle is defined next.

Definition 5. The Minmax-curve circle of an MW-Voronoi region is the smallest circle centered inside or on the boundary of that region, intersecting or touching the region's all boundary curves (or their extensions). This circle is, in fact, $C(\acute{O}_i, \acute{r}_i)$, for the i-th region. It will be shown later that the Minmax-curve circle is not necessarily unique.

Notation 4. The set of all boundary curves of the i-th MW-Voronoi region will hereafter be denoted by ϵ_{i}. In the present subsection (i.e. III-A), intersecting/touching/tangent to a boundary curve ϵ_i means intersecting/touching/tangent to ϵ_i or its extension. It is to be noted that the extension of the boundary curve ϵ_i belongs to the same Apollonian circle as ϵ_i.

Definition 6. The bisector of two curves ϵ_1 and ϵ_2 is defined as the loci of any point E whose distance from ϵ_1 is equal to that from ϵ_2. The bisector of the curves ϵ_1 and ϵ_2 is denoted by $\Gamma_{\epsilon_1,\epsilon_2}$.

Definition 7. Let ϵ_1 and ϵ_2 be the circular arcs of circles C_1 and C_2, respectively. The curves ϵ_1 and ϵ_2 are called parallel if circles C_1 and C_2 are concentric.

A number of lemmas and theorems are presented next as the main results of the paper. The proofs of some lemmas are omitted due to space restrictions, and may be found in [22].

Lemma 1. *Consider two points A, B and a circle $\Omega(O,r)$ (which in particular case can be a straight line). Let the distance between A and $\Omega(O,r)$ be denoted by σ, and that between B and this circle by ρ. Let also the distance between A and B be denoted by ξ. Then:*

$$\sigma - \xi \leq \rho \leq \sigma + \xi \tag{4}$$

Lemma 2. *If an MW-Voronoi region has more than one boundary curve, then the corresponding Minmax-curve circle is tangent to at least two of the boundary curves.*

Definition 8. For any two curves ϵ_1 and ϵ_2, the sets $\Psi^{max}_{\epsilon_1,\epsilon_2}$ and $\Psi^{min}_{\epsilon_1,\epsilon_2}$ are defined as follows:

$$\Psi^{min}_{\epsilon_1,\epsilon_2} = \{X \in \Gamma_{\epsilon_1,\epsilon_2} | \exists \delta > 0 : \quad \forall Y \in \Gamma_{\epsilon_1,\epsilon_2}, |Y - X| \leq \delta \Rightarrow \quad d(X,\epsilon_1) \leq d(Y,\epsilon_1)\} \tag{5}$$

$$\Psi^{max}_{\epsilon_1,\epsilon_2} = \{X \in \Gamma_{\epsilon_1,\epsilon_2} | \exists \delta > 0 : \quad \forall Y \in \Gamma_{\epsilon_1,\epsilon_2}, |Y - X| \leq \delta \Rightarrow \quad d(X,\epsilon_1) \geq d(Y,\epsilon_1)\} \tag{6}$$

Lemma 3. *Consider an MW-Voronoi diagram $\mathcal{V}$, and assume that the i-th region has at least three boundary curves. Then the Minmax-curve circle of this region is tangent to at least two boundary curves. Furthermore, if the Minmax-curve circle is tangent to exactly two boundary curves, say $\acute{\epsilon}_{i1}$ and $\acute{\epsilon}_{i2}$, then at least one of the following conditions hold:*
i) $\acute{\epsilon}_{i1}$ and $\acute{\epsilon}_{i2}$ are parallel;
ii) $\acute{O}_i \in \Psi^{min}_{\acute{\epsilon}_{i1},\acute{\epsilon}_{i2}}$, or
iii) $\acute{O}_i$ is the intersection of the bisector of $\acute{\epsilon}_{i1}$, $\acute{\epsilon}_{i2}$ and one boundary curve of the region.

Lemma 4. *If a Minmax-curve circle is tangent to two parallel curves, then generically there are other Minmax-curve circles, all of which are tangent to these parallel curves, as well.*

Remark 1. Consider an MW-Voronoi region with at least three boundary curves, two of which are parallel. If one of the Minmax-curve circles is tangent to these parallel curves, then genericly all Minmax-curve circles are also tangent to these two curves. At least one of these circles is tangent to some other boundary curves too, and one of such circles is arbitrarily chosen as the Minmax-curve circle in this case.

Definition 9. For convenience of notation, the circle touching two curves ϵ_g and ϵ_h of MW-Voronoi region i, centered at the intersection of the bisector ϵ_g and ϵ_h and the curve ϵ_k, is denoted by $\Omega^k_{g,h}$, for any $k, g, h \in \mathbf{e}_i := \{1, \ldots, e_i\}$. Also, the circle touching two curves ϵ_r and ϵ_s of MW-Voronoi region i, centered at the point $A \in \Psi^{min}_{\epsilon_r,\epsilon_s}$, is denoted by $\Omega^{A,min}_{r,s}$, for any $r, s \in \mathbf{e}_i$.

Theorem 1. *Suppose the i-th MW-Voronoi region has at least three boundary curves. Let $\hat{\mathbf{D}}_i$ and $\grave{\mathbf{D}}_i$ be the sets of all circles $\Omega^k_{g,h}, \forall k, g, h \in \mathbf{e}_i$, and $\Omega^{A,min}_{r,s}, \forall r, s \in \mathbf{e}_i, A \in \Psi^{min}_{\epsilon_r,\epsilon_s}$ such that: (i) their centers lie inside the region or on its boundaries, and (ii) they intersect with or are tangent to all of the boundary curves of the region. Let also $\tilde{\mathbf{D}}_i$ be the set of all circles such that: (i) they are tangent to at least three boundary curves of the i-th MW-Voronoi region (or their extensions); (ii) their centers lie inside the region or on its boundaries, and (iii) they intersect with or are tangent to all of the boundary curves of the MW-Voronoi region (or their extensions). Define $\mathbf{D}_i := \hat{\mathbf{D}}_i \cup \grave{\mathbf{D}}_i \cup \tilde{\mathbf{D}}_i$; then the Minmax-curve circle belongs to $\mathbf{D}_i$, and is the smallest circle in this set.*

Proof: The proof follows directly from Lemmas 3 and 4, Remark 1, and Definitions 5 and 9. ■

Remark 2. If an MW-Voronoi region has exactly one boundary curve, then this curve is a circle and it is considered as the Minmax-curve circle. If, on the other hand, it has exactly two boundary curves, then according to Lemma 2 the Minmax-curve circle is tangent to both curves.

Using the result of Theorem 1 and discussions in Remarks 1 and 2, one can develop a procedure with a complexity of order $O(e_i^3)$ to calculate the Minmax-curve centroid in the i-th MW-Voronoi region. Since typically a MW-Voronoi region does not have "too many" boundary curves, the computational complexity for calculating the Minmax-curve centroid is normally not very high.

B. Maxmin-Curve Strategy

The main idea behind this strategy is that normally for optimal coverage, each sensor should not be too close to any of its Voronoi curves. The Maxmin-curve strategy selects the target location for each sensor as a point inside the corresponding MW-Voronoi region whose distance from the nearest curve is maximized. This point will be referred to as the *Maxmin-curve centroid*, and will be denoted by $\breve{O}_i$ for the i-th region, $i \in \mathbf{n}$. Furthermore, the distance between this point and the nearest curve from it will be represented by $\breve{r}_i$. The Maxmin-curve circle is defined next.

Definition 10. The Maxmin-curve circle of an MW-Voronoi region is the largest circle inside the MW-Voronoi region. This circle is, in fact, $C(\breve{O}_i, \breve{r}_i)$, for the i-th region.

Lemma 5. *If an MW-Voronoi region has more than one boundary curve, then the corresponding Maxmin-curve circle is tangent to at least two of the curves.*

Proof: Let $\breve{\epsilon}_{i1}$ be the nearest boundary curve to the Maxmin-curve centroid of the i-th MW-Voronoi region. This means that $\breve{r}_i$ is equal to the distance between $\breve{O}_i$ and $\breve{\epsilon}_{i1}$, also denoted by $d(\breve{O}_i, \breve{\epsilon}_{i1})$; thus, $C(\breve{O}_i, \breve{r}_i)$ is tangent to $\breve{\epsilon}_{i1}$. Define:

$$\hat{w} = \min_{\epsilon \in \epsilon_{\rm i} - \{\breve{\epsilon}_{i1}\}} \Big\{ d(\breve{O}_i, \epsilon) \Big\} \tag{7}$$

Suppose that the Maxmin-curve circle is not tangent to any other boundary curve, and hence $\delta^* = (\hat{w} - \breve{r}_i)/2$ is strictly positive. Let M be a point on $\breve{\epsilon}_{i1}$ such that $M\breve{O}_i \perp \breve{\epsilon}_{i1}$. Let also $\hat{O}$ be a point on the extension of $M\breve{O}_i$ such that the distance between $\breve{O}_i$ and $\hat{O}$ is equal to an arbitrary value $\delta \in (0, \delta^*]$ (see, e.g. Fig. 3). According to Lemma 1:

$$d(\hat{O}, \epsilon) \geq d(\breve{O}_i, \epsilon) - \delta \geq \hat{w} - \delta, \ \forall \epsilon \in \epsilon_{\rm i} - \{\breve{\epsilon}_{i1}\} \tag{8}$$

From (8) and the relations $\hat{w} - \delta \geq \breve{r}_i + \delta > \breve{r}_i$ and $d(\hat{O}, \breve{\epsilon}_{i1}) > d(\breve{O}_i, \breve{\epsilon}_{i1})$, one can conclude that:

$$\min_{\epsilon \in \epsilon_{\rm i}} \Big\{ d(\hat{O}, \epsilon) \Big\} > \breve{r}_i \tag{9}$$

which contradicts the initial assumption that $\breve{O}_i$ is the Maxmin-curve centroid. This completes the proof. ■

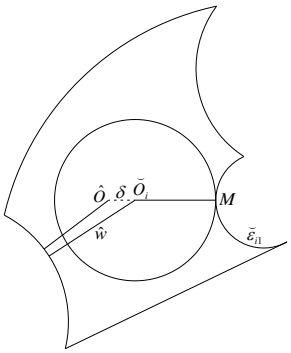

Fig. 3. An illustrative figure used in the proof of Lemma 5.

Lemma 6. *Consider an MW-Voronoi diagram $\mathcal{V}$, and suppose that the i-th MW-Voronoi region has at least three boundary curves. Then the Maxmin-curve circle of this region is tangent to at least three boundary curves. Furthermore, if the Maxmin-curve circle is tangent to exactly two boundary curves, say $\breve{\epsilon}_{i1}, \breve{\epsilon}_{i2}$, then these two curves are either parallel or $\breve{O}_i \in \Psi^{max}_{\breve{\epsilon}_{i1}, \breve{\epsilon}_{i2}}$.*

Proof: Suppose the Maxmin-curve circle of the i-th region is tangent to exactly two curves, say $\breve{\epsilon}_{i1}$ and $\breve{\epsilon}_{i2}$, but these two curves are not parallel. Define:

$$\tilde{w} := \min_{\epsilon \in \epsilon_{\rm i} - \{\breve{\epsilon}_{i1}, \breve{\epsilon}_{i2}\}} \Big\{ d(\breve{O}_i, \epsilon) \Big\} \tag{10}$$

Since $C(\breve{O}_i, \breve{r}_i)$ is tangent to exactly two boundary curves, hence $\delta^* = (\tilde{w} - \breve{r})/2$ is strictly positive. If $\breve{O}_i \notin \Psi^{max}_{\breve{\epsilon}_{i1}, \breve{\epsilon}_{i2}}$, then one can choose a point inside the i-th MW-Voronoi region and on the bisector of $\breve{\epsilon}_{i1}$ and $\breve{\epsilon}_{i2}$, say $\tilde{O}$, such that $d(\tilde{O}, \breve{\epsilon}_{i1}) = d(\tilde{O}, \breve{\epsilon}_{i2}) > \breve{r}_i$, and $\breve{O}_i\tilde{O} = \delta$, for some $\delta \in (0, \delta^*]$ (e.g., see Fig. 4). According to Lemma 1:

$$d(\tilde{O}, \epsilon) \geq d(\breve{O}_i, \epsilon) - \delta \geq \tilde{w} - \delta, \ \forall \epsilon \in \epsilon_{\rm i} - \{\breve{\epsilon}_{i1}, \breve{\epsilon}_{i2}\} \tag{11}$$

It results from (11) and the relations $\tilde{w} - \delta \geq \breve{r}_i + \delta > \breve{r}_i$ and $d(\tilde{O}, \breve{\epsilon}_{i1}) = d(\tilde{O}, \breve{\epsilon}_{i2}) > \breve{r}_i$, that:

$$\min_{\epsilon \in \epsilon_{\rm i}} \Big\{ d(\tilde{O}, \epsilon) \Big\} > \breve{r}_i \tag{12}$$

which contradicts the initial assumption that $\breve{O}_i$ is the Maxmin-curve centroid. This completes the proof. ■

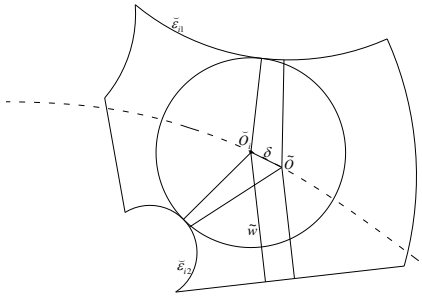

Fig. 4. An illustrative figure used in the proof of Lemma 6.

Definition 11. For convenience of notation, the circle tangent to two curves ϵ_r and ϵ_s of MW-Voronoi region i, centered at the point $A \in \Psi^{max}_{\epsilon_r, \epsilon_s}$, is denoted by $\Omega^{A,max}_{r,s}$ for any $r, s \in \mathbf{e}_i$.

Lemma 7. *If a Maxmin-curve circle is tangent to two parallel curves, then generically there are other Maxmin-curve circles, all of which are tangent to these parallel curves.*

Remark 3. Consider an MW-Voronoi region with at least three boundary curves, two of which are parallel. If one of the Maxmin-curve circles is tangent to these parallel curves, then genericly all Maxmin-curve circles are also tangent to these two curves. At least one of these circles is tangent to some other boundary curves too, and one of such circles is arbitrarily chosen as the Maxmin-curve circle in this case.

Theorem 2. *Consider an MW-Voronoi diagram $\mathcal{V}$, and suppose that the i-th MW-Voronoi region has at least three boundary curves. Let $\grave{\mathbf{Z}}_i$ be the set of all circles $\Omega^{A,max}_{r,s}, \forall r, s \in \mathbf{e}_i, A \in \Psi^{max}_{\epsilon_r, \epsilon_s}$ that are inside the region. Let also $\tilde{\mathbf{Z}}_i$ be the set of all circles which: (i) are tangent to at least three curves of region i, and (ii) are inside the region. Define $\mathbf{Z_i} := \grave{\mathbf{Z}}_\mathbf{i} \cup \tilde{\mathbf{Z}}_\mathbf{i}$; then the Maxmin-curve circle belongs to $\mathbf{Z}_i$, and also it is the largest circle in this set.*

Proof: The proof follows directly from Lemmas 6 and 7, Definitions 10 and 11, and Remark 3. ■

Remark 4. If the MW-Voronoi region has exactly one boundary curve, then this curve is a circle as pointed out before, and it is, in fact, the Maxmin-curve circle.

Using the result of Theorem 2 and discussion in Remarks 3 and 4, one can develop a procedure with a complexity of order $O(e_i^3)$ (which is typically not very high) to calculate the Maxmin-curve centroid for the i-th MW-Voronoi region, $i \in \mathbf{n}$.

C. Curtex Strategy

By properly combining the strategies introduced in the previous subsection and existing techniques, one can come up with more efficient algorithms for coverage. This improvement, however, comes at the expense of more involved computation for the destination point. The Curtex method introduced here is a combination of the Maxmin-curve strategy proposed in this paper, and the Minmax-vertex strategy

introduced in [22]. In this method, every sensor finds two points in each round as its new location: one point according to the Maxmin-curve strategy, and another one according to the Minmax-vertex strategy. One of the two points which provides better coverage is subsequently selected as the target location of the sensor. Simulation results in the next section demonstrate that this algorithm outperforms the other strategies in terms of coverage.

Remark 5. In some special cases, even if the sensor moves toward its target location (according to any of the algorithms introduced above), the local coverage might not be improved. This happens when the target location is too far from its present location. To overcome this problem, one can adopt a technique similar to the one provided in [12], and choose the midpoint or $3/4$ point between the current location and the calculated target location. If the local coverage of the sensor is better from this point (compared to the calculated target point), it stops there.

Remark 6. In order to prevent the sensors from oscillatory movements, a proper scheme can be used to let each sensor move toward the target location only if the direction of its move is consistent with its move in the preceding round, as proposed in [12].

IV. Simulation Results

In this section, the three algorithms proposed in Section III are applied to a flat space of size $50\text{m}\times 50\text{m}$. It is to be noted that the results presented in this section for field coverage are all the average values obtained by using 20 random initial deployments for the sensors. Furthermore, while the horizontal axis in all figures in this section represents a discrete parameter, the graphs are displayed as continuous curves for clarity.

Assume first there are 36 sensors: 20 with a sensing radius of 6m, 8 with a sensing radius of 5m, 4 with a sensing radius of 7m, and 4 with a sensing radius of 9m. Moreover, the communication range of each sensor is assumed to be $10/3$ times greater than its sensing range. The coverage factor (defined as the ratio of the covered area to the overall area) of the sensors in each round is depicted in Fig. 5 for the algorithms proposed in this paper. It can be seen from this figure that all three algorithms result in a satisfactory coverage level of the target field in the first few rounds. It can also be observed that for this example the Curtex algorithm performs better than the other algorithms as far as coverage is concerned.

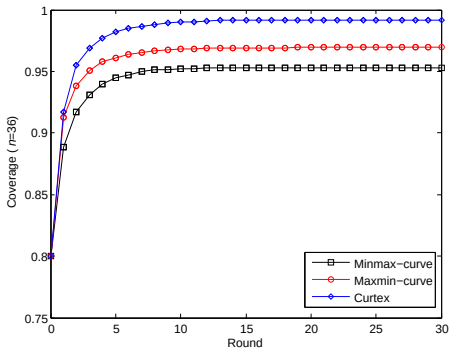

Fig. 5. Network coverage per round for 36 sensors.

It is desired now to compare the performance of the proposed algorithms in terms of the number of deployed sensors n. To this end, consider three more set-ups: n=18, 27, and 45, in addition to the set-up discussed above. Let the changes in the number of identical sensors in the new setups be proportional to the changes in the total number of sensors (e.g., for the case of n=18 there will be 10 sensors with a sensing radius of 6m, 4 with a sensing radius of 5m, 2 with a sensing radius of 7m, and 2 with a sensing radius of 9m). Fig. 6 provides the coverage results for different number of sensors. It can be seen from this figure that the target field coverage in Curtex algorithm is larger than that in other two algorithms for different number of sensors.

Another important factor in the performance evaluation of different algorithms is how fast the desired coverage level is achieved. Notice that the sensor deployment time in each round is almost equal for all algorithms. Hence, to compare the deployment speed, it suffices to check the number of rounds it takes for the sensors to provide a prescribed coverage level. It is shown in Fig. 7 that in all three algorithms the number of rounds (required to meet a certain termination condition) increases by increasing the number of sensors up to a certain value, and then starts to decrease by adding more sensors. This is due mainly to the fact that when there are a small number of sensors in the target field, the MW-Voronoi regions are large in comparison with the corresponding sensing circles. Hence, there is a good chance that each sensor's local coverage area is completely inside its MW-Voronoi region, which means that the sensor does not need to move in order to increase its coverage area. On the other hand, when there are a large number of sensors in the target field, there is a good chance that each sensor covers its MW-Voronoi region, which implies that the termination condition will be satisfied in a short period of time. It is also to be noted that the number of rounds in the Minmax-curve algorithm is relatively low, making it a good candidate for field coverage as far as deployment time is concerned.

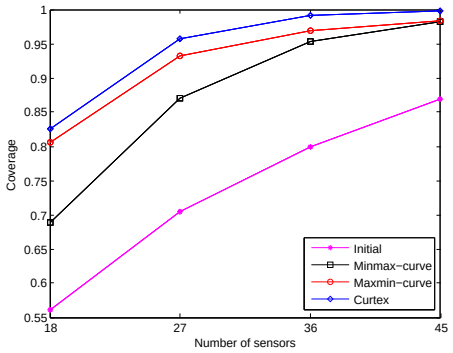

Fig. 6. Network coverage for different number of sensors using the proposed algorithms.

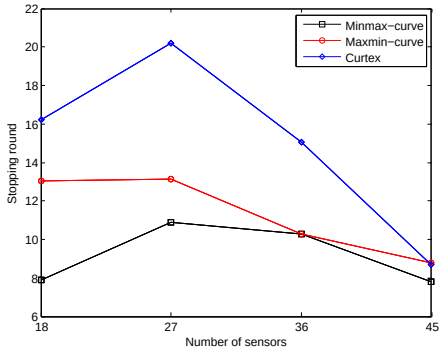

Fig. 7. The number of rounds required to reach the termination conditions for different number of sensors using the proposed algorithms.

Another important means of assessing the performance of sensor deployment algorithms is the energy consumption of the sensors. Sensors' energy consumption highly depends on the traveling distance of sensors, and the number of times they stop before arriving at the destination (the latter is due to static friction). Thus, to compare the proposed methods in terms of energy consumption, the traveling distance and the number of movements should be taken into consideration. Fig. 8 depicts the average moving distance for different number of sensors. This figure shows that by increasing the number of sensors, the average moving distance of the sensors is decreased in all scenarios. This is due to the fact that in all algorithms when the number of sensors increases, the MW-Voronoi regions become smaller. As a result, the distance between each sensor and its destination point in the corresponding MW-Voronoi region decreases, which leads to a decrease in the average moving distance. It can be seen from Fig. 8 that the average moving distance of all three algorithms are more or less the same when there are large number of sensors in the field. The number of movements versus the number of sensors is depicted in Fig. 9. It can be observed from this figure that when the number of sensors is more than a certain level (whose value varies for different algorithms), the number of movements decreases. This is due to the fact that for large number of sensors the MW-Voronoi regions become smaller, and hence the sensors will likely cover their MW-Voronoi regions. As a result, the coverage holes will be covered in a shorter period of time, decreasing the number of movements.

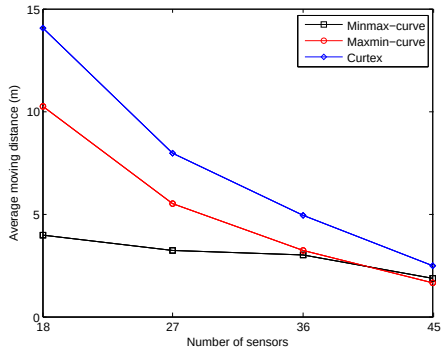

Fig. 8. The average distance each sensor travels for different number of sensors using the proposed algorithms.

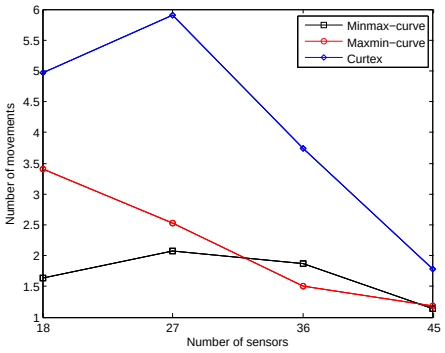

Fig. 9. The number of movements required for different number of sensors using the proposed algorithms.

V. Conclusions

This paper presents efficient deployment algorithms for field coverage in a network of mobile sensors with different sensing ranges. A multiplicatively weighted Voronoi (MW-Voronoi) diagram is then employed to develop three distributed deployment algorithms accordingly. Under these algorithms, the sensors move iteratively to minimize coverage holes in the network. The algorithms are based on some known facts about the general characteristics of an ideal sensor configuration (e.g., each sensor should not be too far or too close to any of the boundary curves of its corresponding MW-Voronoi region). Simulation results are pretested to compare the proposed approaches for different number of sensors in the network in terms of coverage factor and energy consumption (which is assumed to be mainly a function of number of stops as well as moving distance).

References

[1] C. Intanagonwiwat, R. Govindan, and D. Estrin, "Directed diffusion: A scalable and robust communication paradigm for sensor networks," in *Proceedings of the 6th Annual International Conference on Mobile Computing and Networking*, 2000, pp. 56–67.

[2] G. J. Pottie and W. J. Kaiser, *Wireless Integrated Network Sensors*. ACM New York, NY, USA, 2000.

[3] K. Sohrabi, J. Gao, V. Ailawadhi, and G. J. Pottie, "Protocols for self-organization of a wireless sensor network," *IEEE Personal Communications*, vol. 7, pp. 16–27, 2000.

[4] H. Mahboubi, A. Momeni, A. G. Aghdam, K. Sayrafian-Pour, and V. Marbukh, "Optimal target tracking strategy with controlled node mobility in mobile sensor networks," in *Proceedings of American Control Conference*, 2010, pp. 2921–2928.

[5] H. Mahboubi, K. Moezzi, A. G. Aghdam, K. Sayrafian-Pour, and V. Marbukh, "Self-deployment algorithms for coverage problem in a network of mobile sensors with unidentical sensing range," in *Proceedings of IEEE Global Communications Conference*, 2010, to appear.

[6] A. Howard, M. J. Matarić, and G. S. Sukhatme, "An incremental self-deployment algorithm for mobile sensor networks," *Autonomous Robots*, vol. 13, pp. 113–126, 2002.

[7] T. Clouqueur, V. Phipatanasuphorn, P. Ramanathan, and K. K. Saluja, "Sensor deployment strategy for detection of targets traversing a region," *ACM Mobile Networks and Applications*, vol. 8, pp. 453–461.

[8] X. Li, A. Nayak, and I. Stojmenovic, "Location service in sensor and mobile actuator networks," *Wireless Sensor and Actuator Networks: Algorithms and Protocols for Scalable Coordination and Data Communication*, p. 209, 2010.

[9] M.-C. Zhao, J. Lei, M.-Y. Wu, Y. Liu, and W. Shu, "Surface coverage in wireless sensor networks," in *Proceedings of the 28th IEEE INFOCOM*, 2009, pp. 109–117.

[10] A. Boukerche and X. Fei, "A voronoi approach for coverage protocols in wireless sensor networks," in *Proceedings of IEEE Global Communications Conference*, 2007, pp. 5190–5194.

[11] G. Wang, G. Cao, P. Berman, and T. F. L. Porta, "A bidding protocol for deploying mobile sensors," *IEEE Transactions on Mobile Computing*, vol. 6, pp. 563–576, 2007.

[12] G. Wang, G. Cao, and T. F. L. Porta, "Movement-assisted sensor deployment," *IEEE Transactions on Mobile Computing*, vol. 5, pp. 640–652, 2006.

[13] J. Luo and Q. Zhang, "Probabilistic coverage map for mobile sensor networks," in *Proceedings of IEEE Global Communications Conference*, 2008, pp. 357 – 361.

[14] A. Konstantinidis, K. Yang, and Q. Zhang, "An evolutionary algorithm to a multi-objective deployment and power assignment problem in wireless sensor networks," in *Proceedings of IEEE Global Communications Conference*, 2008, pp. 475 – 480.

[15] E. Deza and M. M. Deza, *Encyclopedia of Distances*. Springer, 2009.

[16] A. Okabe, B. Boots, K. Sugihara, and S. N. Chiu, *Spatial Tessellations: Concepts and Applications of Voronoi Diagrams*. Wiley, 2000.

[17] R. Reitsma, S. Trubin, and E. Mortensen, "Weight-proportional space partitioning using adaptive voronoi diagrams," *Geoinformatica*, vol. 11, pp. 383–405, 2007.

[18] A. V. Akopyan and A. A. Zaslavsky, *Geometry of Conics*. American Mathematical Society, 2007.

[19] D. E. Koditschek, *Robot Planning and Control via Potential Functions*. MIT Press Cambridge, MA, USA, 1989.

[20] Q. Li, M. D. Rosa, and D. Rus, "Distributed algorithms for guiding navigation across a sensor network," in *Proceedings of the 9th Annual International Conference on Mobile Computing and Networking*, 2003, pp. 313–325.

[21] D. Niculescu and B. Nath, "Ad hoc positioning system (aps) using aoa," in *Proceedings of IEEE INFOCOM. Twenty-Second Annual Joint Conference of the IEEE Computer and Communications Societies*, 2003, pp. 1734–1743.

[22] H. Mahboubi, K. Moezzi, A. G. Aghdam, and K. Sayrafian-Pour, "Self-deployment algorithms for coverage problem in a network of mobile sensors with unidentical sensing range," *Concordia University Technical Report*, 2010 (available online at www.ece.concordia.ca/∼aghdam/TechnicalReports/techrep2010_3.pdf).